INTERNATIONAL JOURNAL FOR NUMERICAL METHODS IN FLUIDS, VOL. 5, 331–345 (1985)

A COMPATIBLE MIXED DESIGN AND ANALYSIS FINITE ELEMENT METHOD FOR THE DESIGN OF TURBOMACHINERY BLADES

R. D. CEDAR* AND P. STOW†

Rolls-Royce Limited, P.O. Box 31, Derby DE2 8BJ, England

SUMMARY

In this paper the development of a compatible mixed design and analysis method is presented for the quasi-three-dimensional finite element blade-to-blade program FINSUP. The method consists of two parts. The first is concerned with a method of modelling changes to a blade shape using a surface transpiration model. The second is concerned with determining the relationship between the displaced blade surface and the surface velocity distribution. It is shown that with the Newton–Raphson procedure adopted in the method a very efficient manner of introducing the design option is possible. As a consequence the resulting program is fast and completely interactive. A number of examples are given to illustrate how the mixed design and analysis mode can be used in practical blade design.

KEY WORDS Turbomachines Design Finite Element

INTRODUCTION

Traditionally turbomachinery blade design has been based on Wu's[1] approach to solving the three-dimensional flow equations using quasi-three-dimensional through-flow and blade-to-blade analyses. The through-flow calculation provides the inlet conditions, the mass flow passing through the blade row and the turning that the blades must achieve. The designer's objectives are to produce blade sections that satisfy these conditions, and any additional geometric conditions imposed, for example by stress or cooling considerations, while achieving an acceptable efficiency for the blade row. The demand for more efficient gas turbines has led to greater care in the design of blade sections to reduce losses. This has been achieved by removing loss producing features such as shocks and rapid diffusions, so avoiding boundary layer separations.

There are two basic approaches for blade design that can be adopted, namely using a design program or an analysis program. With a pure design program the input is a desired surface velocity distribution and the output from the program is the blade geometry that gives rise to this; examples are References 2–4. Often such methods are either two-dimensional or are limited in their handling of quasi-three-dimensional (streamtube height, streamline radius and blade rotation) effects. It is also difficult to achieve mixed geometric and aerodynamic constraints that often occur. With an analysis method the input is the blade geometry and output is the surface velocity distribution. There are many analysis methods available that account accurately for the quasi-three-dimensional effects and have few restrictions.

*Senior Theoretical Scientist
†Head of Theoretical Science Group

0271–2091/85/04 0331–15$01.50

Received 2 February 1984
Revised 6 June 1984

Use of an analysis method makes the achievement of geometric constraints easier but now the designer has to modify the blade geometry and re-analyse the blade in order to achieve the desired velocity distribution; this becomes tedious and slow. The efficiency of the process can be greatly increased if the analysis method has a compatible design option. With such a mixed design and analysis method the designer is able to specify part of the geometry and part of the surface velocity distribution so that both aerodynamic and structural requirements can be achieved.

In this paper the development of a compatible mixed design and analysis method is presented for the inviscid, quasi-three-dimensional finite element blade-to-blade program FINSUP reported in References 5–7. The method consists of two parts. The first is concerned with a method of modelling changes to a blade shape using a surface transpiration model. The second is concerned with determining the relationship between the displaced blade surface and the surface velocity distribution. It is shown that with the Newton–Raphson procedure adopted in the method a very efficient manner of introducing the design option is possible. As a consequence the resulting program is fast and completely interactive. A number of examples are given to illustrate how the mixed design and analysis mode can be used in practical blade design.

TRANSPIRATION MODEL

In this section the problems of modelling the effects on the surface velocity distribution from changes to the blade geometry are considered. There are two possible approaches. The direct method is to calculate the new blade shape and re-analyse the flow. In general, this involves reconstructing the mesh, which for a finite element method can be time-consuming. A typical mesh is shown in Figure 1. An alternative approach is to model the displacement of the blade by transpiration of fluid through the original blade surface. This has the advantages that the mesh

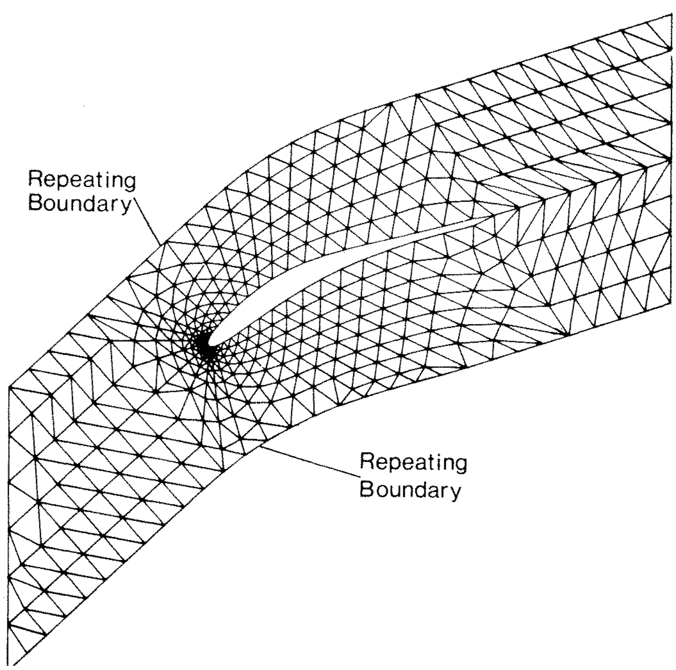

Figure 1. Typical finite element mesh

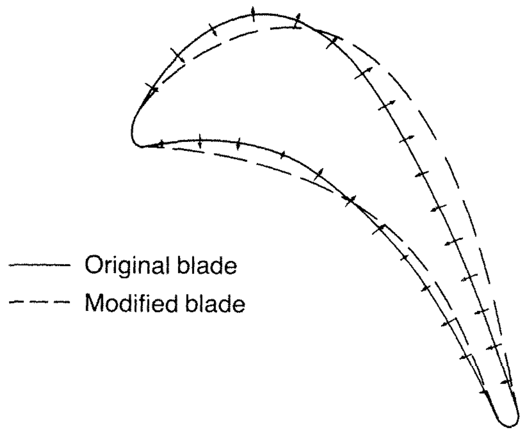

Figure 2. Blade surface displacement by transpiration

does not have to be reconstructed and the flow solution for the original blade can be used as the starting conditions for the modified blade.

In the transpiration model displacements of the blade are accounted for by injection of fluid through the original blade surface. The original blade surface is no longer a streamline (see Figure 2). The transpiration velocity (see Figure 3) can be related to changes in the displacement of the blade. From Figure 3 we have

$$\int_{\mathrm{A}}^{\mathrm{B}} \rho W_n h \, \mathrm{d}S = \int_0^{\xi_{\mathrm{B}}} \rho W_S h \, \mathrm{d}n - \int_0^{\xi_{\mathrm{A}}} \rho W_S h \, \mathrm{d}n \tag{1}$$

where h is the streamtube height.

Expanding the terms on the R.H.S. as a Taylor series about the original blade position gives:

$$\begin{aligned} \int_{\mathrm{A}}^{\mathrm{B}} \rho W_n h \, \mathrm{d}S &= \int_0^{\xi_{\mathrm{B}}} \left\{ (\rho W_S h) + n \frac{\partial}{\partial n}(\rho W_S h) \right\}_{\mathrm{B}} \mathrm{d}n \\ &\quad - \int_0^{\xi_{\mathrm{A}}} \left\{ (\rho W_S h) + n \frac{\partial}{\partial n}(\rho W_S h) \right\}_{A} \mathrm{d}n \\ &= (\rho W_S h)_{\mathrm{B}} \xi_{\mathrm{B}} - (\rho W_S h) \xi_{\mathrm{A}} \\ &\quad + \left[\frac{\partial}{\partial n}(\rho W_S h) \frac{\xi^2}{2} \right]_{\mathrm{B}} - \left[\frac{\partial}{\partial n}(\rho W_S h) \frac{\xi^2}{2} \right]_{A} \end{aligned} \tag{2}$$

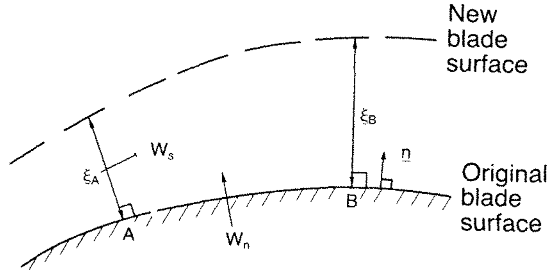

Figure 3. Transpiration velocity used to model blade displacement

where the subscripts A and B refer to the values at the original blade surface and where higher order terms in the expansion are neglected. It can be shown that along a normal to the blade surface

$$\frac{\partial}{\partial n}(\rho W_S) \approx \rho W_S \kappa \tag{3}$$

where κ is the blade surface curvature. Substituting equation (3) into equation (2), then as $A \to B$

$$\rho W_n h = \frac{\mathrm{d}}{\mathrm{d}S}(\rho W_S h \xi^*) \tag{4}$$

where

$$\xi^* = \xi(1 + \tfrac{1}{2}\kappa) \tag{5}$$

The term $\frac{1}{2}\xi\kappa$ can be considered as a correction to the element displacement due to curvature. This term is only significant if the blade displacement is of the same order as the local radius of curvature, for example if large changes are made around the leading edge of a blade. In the subsequent analysis the * superscript is dropped. It should be noted that in practice W_S is taken as the total relative velocity W.

TRANSPIRATION MASS FLOW

The transpiration mass flow used to model blade displacements can be incorporated in the finite element formulation through the boundary conditions. The continuity equation for steady flow in a co-ordinate system which is rotating with the blade is

$$\nabla \cdot \rho \mathbf{W} h = 0 \tag{6}$$

where $\mathbf{W}$ is the relative velocity vector. The weighted residual procedure gives for each node (I) where the solution is required

$$\iint (\nabla \cdot \rho \mathbf{W} h) G_I \, \mathrm{d}A = 0 \tag{7}$$

where G_I is a global weighting function associated with node I. From equation (7) we have

$$\iint (\nabla \cdot \rho \mathbf{W} h G_I - \rho \mathbf{W} h \cdot \nabla G_I) \mathrm{d}A = 0$$

or

$$\iint \rho \mathbf{W} h \cdot \nabla G_I \mathrm{d}A = -\int \rho \mathbf{W} h G_I \cdot \mathbf{n} \, \mathrm{d}S$$

$$= -\int \rho W_n h G_I \, \mathrm{d}S \tag{8}$$

$\mathbf{n}$ being the local inward normal and S the perimeter of the domain of integration being positive in an anti-clockwise direction.

In the Galerkin weighted residual form, where G_I is replaced locally by the shape function N_I in each element, equation (8) becomes

$$\sum_{e(I)} \iint \rho \mathbf{W} h \cdot \nabla N_I \, \mathrm{d}A = -\sum_{e(I)} \int \rho W_n h N_I \, \mathrm{d}S \tag{9}$$

where the summations are over all elements containing I as a node. The line integral in equation (9) occurs only on the domain boundary, i.e. inlet and exit planes and the blade surface. In the case of no displacement of the blade surface or inclusion of a boundary layer, the blade surface boundary condition is

$$W_n = 0$$

and the only line integrals to occur are at the inlet and exit. In the case where the blade shape has been modified by transpiration then W_n is non-zero, being related to the blade displacement by equation (4), and a line integral is needed for the surface nodes corresponding to the parts of the blade that have been modified.

BLADE SURFACE INTEGRALS

By substituting equation (4) into equation (9) the blade surface integral becomes

$$\begin{aligned} T &= -\sum_{e(I)} \int \frac{\mathrm{d}}{\mathrm{d}S}(\rho W h \xi) N_I \,\mathrm{d}S \\ &= -\sum_{e(I)} \left\{ [\rho W h \xi N_I]_{\mathrm{A}}^{\mathrm{B}} - \int \rho W h \xi \frac{\mathrm{d}N_I}{\mathrm{d}S} \mathrm{d}S \right\} \end{aligned} \tag{10}$$

where element nodes A and B are defined in Figure 4. Considering node B, for element ABC

$$N_I = \begin{cases} 0 \text{ at node A} \\ 1 \text{ at node B} \end{cases}$$

for element BDE

$$N_I = \begin{cases} 1 \text{ at node B} \\ 0 \text{ at node D} \end{cases}$$

Then

$$T = \sum_{e(I)} \int \rho W h \xi \frac{\mathrm{d}N_I}{\mathrm{d}S} \mathrm{d}S \tag{11}$$

For a 3-node triangle we have

$$\begin{aligned} \frac{\mathrm{d}N_I}{\mathrm{d}S} &= \frac{1}{S_{\mathrm{AB}}}, \quad \text{for element ABC} \\ &= \frac{-1}{S_{\mathrm{BD}}}, \quad \text{for element BDE} \end{aligned}$$

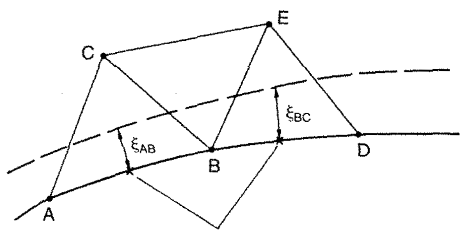

Figure 4. Geometry of surface elements

In the case of a quasi-three dimensional analysis where ρ and W vary over an element we replace them by element mean quantities, see reference 7, so that

$$\begin{aligned} T &\approx \sum_{e(I)} \rho^{\mathrm{m}} W^{\mathrm{m}} h^{\mathrm{m}} \frac{\mathrm{d}N_I}{\mathrm{d}S} \int \xi \, \mathrm{d}S \\ &= \sum_{e(I)} \rho^{\mathrm{m}} W^{\mathrm{m}} h \bar{\xi} \end{aligned} \tag{12}$$

Where the superscript 'm' denotes an element mean quantity and where for example

$$\bar{\xi}_{\mathrm{AB}} = \frac{1}{S_{\mathrm{AB}}} \int_{\mathrm{A}}^{\mathrm{B}} \xi \, \mathrm{d}S$$

Dropping the superscript notation gives

$$T = [(\rho W h \xi)_{\mathrm{AB}} - (\rho W h \xi)_{\mathrm{BD}}] \tag{13}$$

Equation (13) may be written in matrix form as

$$\mathbf{T} = \mathbf{B}\boldsymbol{\xi} \tag{14}$$

where $\mathbf{T}$ is an N element column vector containing the transpiration integral for the N nodes on the blade surface. The transpired fluid can be thought of as entering uniformly through the surface of the element. $\mathbf{B}$ is an $N \times M$ bi-diagonal matrix where M is the number of elements on the blade surface. $\boldsymbol{\xi}$ is a column vector containing the normal displacement of every surface element. At points where no change to the original blade is desired, for example to satisfy a geometric constraint, then the corresponding element of $\boldsymbol{\xi}$ is zero.

INCLUSION OF TRANSPIRATION IN THE SOLUTION SCHEME

The flow is taken as being steady in a co-ordinate system rotating with the blade. In reference 7 it is shown that for isentropic flow a velocity potential (ϕ) can be introduced such that

$$\nabla\phi = \mathbf{W} + \boldsymbol{\Omega} \times \mathbf{R} \tag{15}$$

where $\mathbf{W}$ is the velocity relative to the blade, $\boldsymbol{\Omega}$ the rotational speed of the blade and $\mathbf{R}$ the streamline radius.

Equation (9) is applied at each node of the flow domain leading to a set of non-linear equations that may be written as

$$\mathbf{A}(\boldsymbol{\phi}) = \mathbf{C} + \mathbf{B}^*\boldsymbol{\xi} \tag{16}$$

Where $\mathbf{A}$ is an N element column vector, N now being the total number of nodes in the solution domain. $\mathbf{C}$ is a column vector formed from only inlet and exit conditions. The matrix $\mathbf{B}^*$ is an expansion of the matrix $\mathbf{B}$ in equation (14), to include all nodes, but only rows corresponding to nodes on the blade surface are non-zero. The matrix $\mathbf{B}^*$ depends on velocity potential, i.e.

$$\mathbf{B}^* = \mathbf{B}^*(\boldsymbol{\phi})$$

An iterative procedure is adopted for the solution of equation (16) which may be written as

$$\mathbf{A}(\boldsymbol{\phi}^{n+1}) = \mathbf{C} + \mathbf{B}^*(\boldsymbol{\phi}^n)\boldsymbol{\xi} \tag{17}$$

where the superscript n denotes the nth approximation to the solution. A Newton–Raphson procedure is adopted[5,6] in which

$$\boldsymbol{\phi}^{n+1} = \boldsymbol{\phi}^n + \boldsymbol{\phi}'$$

giving

$$\mathbf{J}(\boldsymbol{\phi}^n)\boldsymbol{\phi}' = \mathbf{C} - \mathbf{A}(\boldsymbol{\phi}^n) + \mathbf{B}^*(\boldsymbol{\phi}^n)\xi \tag{18}$$

Where $\mathbf{J}$ is the Jacobian matrix

$$J_{ij} = \frac{\partial A_i}{\partial \phi_j} \tag{19}$$

Equation (18) is solved for $\boldsymbol{\phi}'$ using a Gaussian elimination technique. The value of velocity potential at each node is then updated and the equations resolved. This is repeated until convergence is obtained.

RELATIONSHIP BETWEEN MACH NUMBER DISTRIBUTION AND BLADE DISPLACEMENT

Suppose we have a solution $\bar{\boldsymbol{\phi}}$ for the original blade, then a change ξ' to the blade displacement produces a change $\boldsymbol{\phi}'$ to the velocity potential related from equation (18), by

$$\mathbf{J}(\bar{\boldsymbol{\phi}})\boldsymbol{\phi}' = \mathbf{B}^*(\bar{\boldsymbol{\phi}})\xi' \tag{20}$$

where $\bar{\boldsymbol{\phi}}$ satisfies

$$\mathbf{A}(\bar{\boldsymbol{\phi}}) = \mathbf{C} + \mathbf{B}^*\bar{\xi} \tag{21}$$

The change in the surface velocity can be related to the change in potential by

$$\mathbf{W}' = \mathbf{D}\boldsymbol{\phi}'$$

Consequently

$$\begin{aligned} \mathbf{W}' &= \mathbf{D}\mathbf{J}^{-1}\mathbf{B}^*\xi' \\ &= \mathbf{K}\xi' \end{aligned} \tag{22}$$

where $\mathbf{K}$ is referred to as the influence matrix and gives the influence of the blade shape on the surface Mach number distribution. It remains to determine $\mathbf{K}$. It can be seen that if in equation (22) we replace ξ' by

$$\xi' = \xi(0 \cdots 0, 1, 0 \cdots 0)$$

where the 1 is the jth element, then

$$K_{ij} = W_i', \quad \text{for all nodes } i \tag{23}$$

i.e. the elements of the jth column of $\mathbf{K}$ are given by the velocity perturbations produced by transpiration for the jth element only. By taking $j = 1, 2, \ldots, M$ in turn, i.e. by displacing each element of the blade individually, the elements of the $\mathbf{K}$ matrix can be found. It can be seen from equation (20) that the procedure can be carried out very efficiently by using a series of right-hand sides in equation (20).

Inverting $\mathbf{K}$ gives the influence of changes of velocity (and therefore Mach number) on the blade shape

$$\xi' = \mathbf{K}^{-1}\mathbf{W}' \tag{24}$$

where

$$\mathbf{W}' = \mathbf{W}_R - \mathbf{W} \tag{25}$$

$\mathbf{W}_R$ being the required velocity distribution and $\mathbf{W}$ the velocity distribution around the original blade. Equation (22) assumes that the velocity varies linearly with blade displacement and

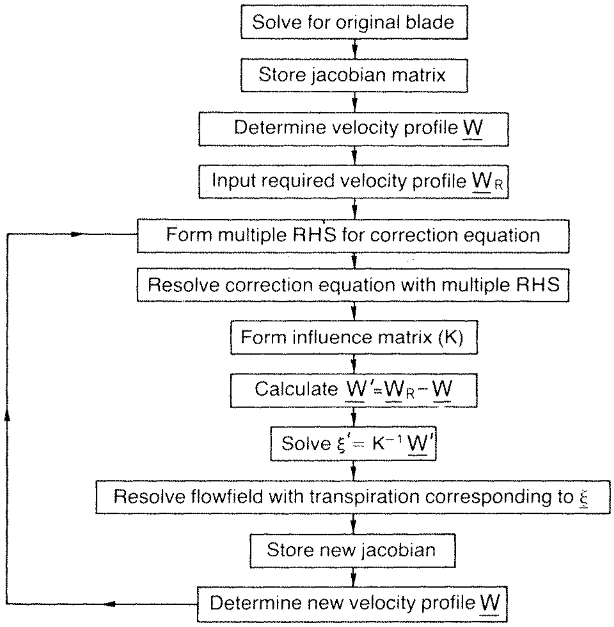

Figure 5. Flow diagram of solution procedure

therefore ξ is only an approximation to the displacement required to obtain $\mathbf{W}_R$. To obtain the exact displacement this process must be repeated in an iterative procedure. A flow diagram of this process is given in Figure 5.

EXAMPLES OF THE USE OF THE DESIGN MODE

The design method has been incorporated into the finite element program FINSUP. The accuracy of the analysis mode of the program has been demonstrated for subsonic, transonic and supersonic flows in References 6 and 7. It is shown in Reference 6 how an upwinding technique can be used to capture shock waves. The addition of the design mode allows the designer to interactively modify the Mach number distribution allowing part of the blade to move, while the geometry of other parts of the blade can be kept fixed. The following examples show the validity of the model and how it is used to solve current problems in the design of gas turbine blades.

1. *Flat plate to DCA test case*

This test case has been included to demonstrate the validity of the design method. To do this the 'first guess' was a cascade of flat plates with an inlet Mach number of 0·5. The desired Mach number distribution corresponded to that of a double circular arc (DCA) blade with no stagger, a thickness chord ratio of 0·05 and the same inlet Mach number. Figure 6 shows the profile of the DCA blade and the design mode approximations to this after the first three iterations. From this it can be seen that after three iterations the design procedure produces a blade with a geometry that is within an acceptable tolerance of the double circular arc blade. If further iterations were performed differences in the blade shape would be reduced. This example verifies that transpiration can be used to model blade displacement and that the design mode will converge to the correct solution in a small number of iterations.

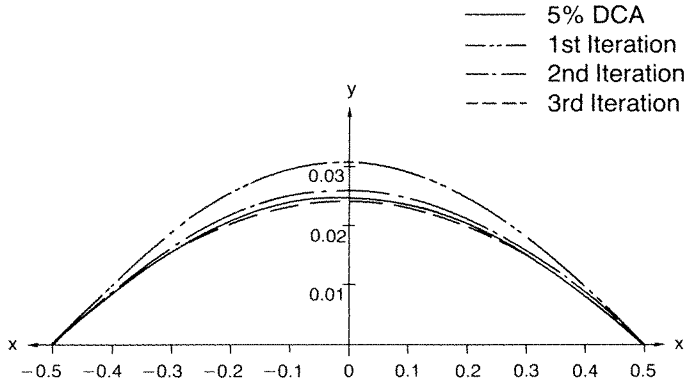

Figure 6. Convergence of the design mode

2. The redesign of a BGK type supercritical compressor blade

The design of transonic shock free compressor blades with controlled diffusion to avoid boundary layer separation was first achieved using the Hodograph method of Bauer, Garabedian and Korn.[2] The suction surface Mach number distribution is characterized by a very steep acceleration at the leading edge followed by an area of supersonic flow at near constant Mach numbers, before the controlled diffusion to subsonic exit flow. An example of this is shown in Figure 7. The work of Rechter et al.[8] and Schmidt[4] has suggested that significant improvements in efficiency can be achieved by moving to a 'laid-back' velocity distribution with a less severe leading edge acceleration (see Figure 7).

In this example a BGK type blade is analysed (Figure 8) and the Mach number distribution modified to reduce the leading edge acceleration. By keeping the area enclosed by the blade surface pressure distribution constant, the work done by the blade has not been changed. Figure 9 shows the Mach number around the modified blade with transpiration to model the blade displacement and Figure 10 indicates the change in the blade shape that results. In order to check that the transpiration models the actual blade displacemeant, a mesh was constructed around the modified blade and the flow re-analysed. The resulting Mach number distribution was exactly the same as that obtained by transpiration.

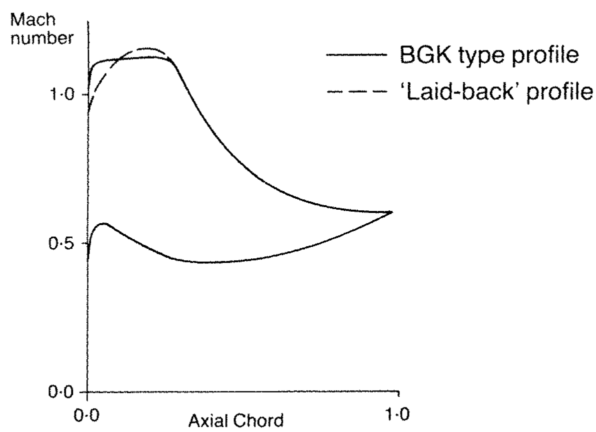

Figure 7. BGK and 'laid-back' type Mach number distribution

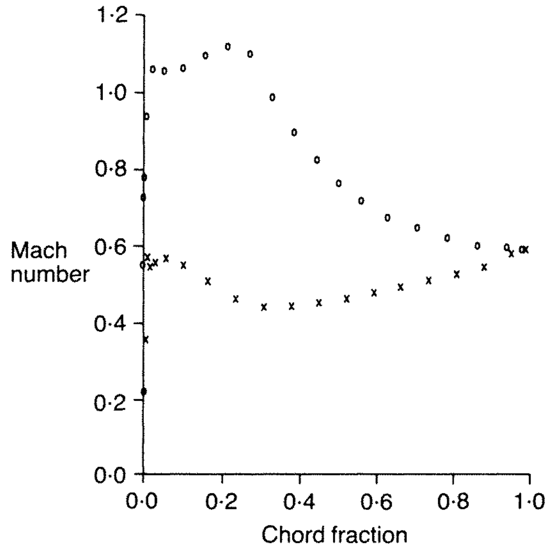

Figure 8. Mach number distribution around original BGK type blade

3. *The redesign of a transonic compressor blade to remove a shock*

Sobieczky and Dulikravich[9] have recently published details of a method that can be used to design shock free turbomachinery blades. A fictitious gas approach is used to determine the extent of a supersonic patch and in particular the position of the sonic line. Using the method of characteristics within the supersonic patch the blade surface geometry can be determined to ensure that the patch is shock free; this has been used with success in a number of cases. There is, however no guarantee that the suction surface diffusion on the resulting blade is not so great that turbulent separation of the boundary layer will occur, and so it is possible that improved efficiencies can be obtained from consideration of this area.

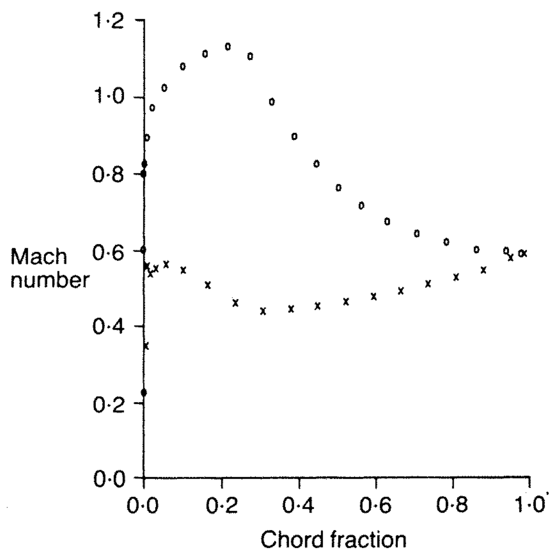

Figure 9. Designed 'laid-back' type blade

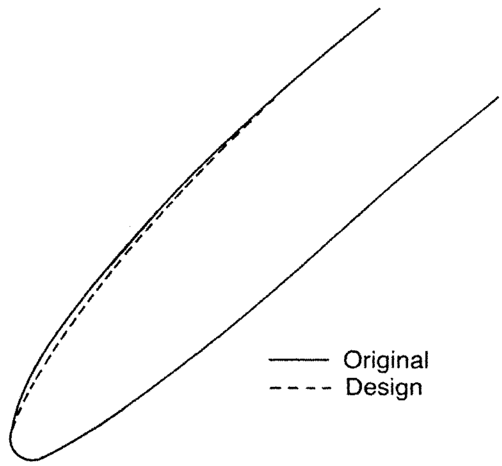

Figure 10. Change in blade shape to reduce leading edge acceleration

In the example considered here it is shown that the design method can be used to redesign a compressor blade to remove a shock. A shock such as that shown in Figure 11 would be considered undesirable because the associated shock loss and the resulting boundary layer thickening or separation would reduce the efficiency of the compressor. Because the required Mach number distribution can be supplied, the designer can ensure that boundary layer separation will not occur. Figure 11 shows a BGK type blade run at an inlet Mach number above design resulting in a shock at 35 per cent axial chord on the suction surface. The Mach number distribution has been modified to remove the shock and after 4 iterations of the design procedure the required Mach number distributions is achieved (Figure 12). The resulting changes in the blade shape are shown in Figure 13.

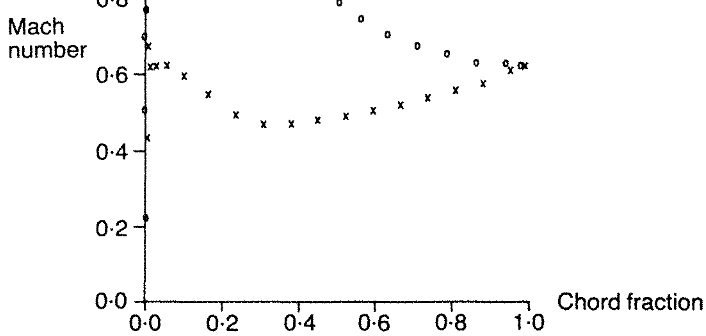

Figure 11. Supercritical compressor blade with shock

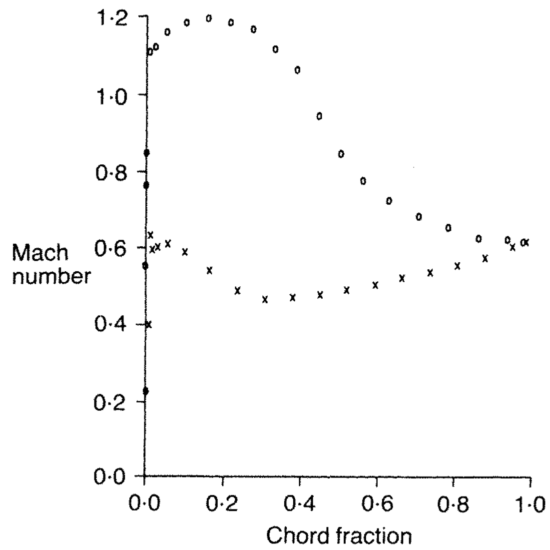

Figure 12. Design Mach number distribution

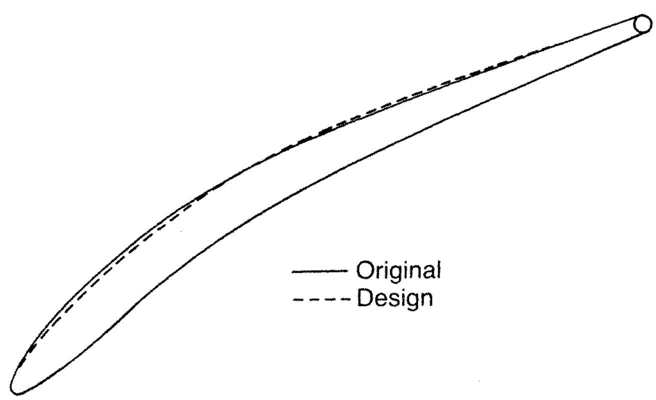

Figure 13. Change in blade shape to remove shock

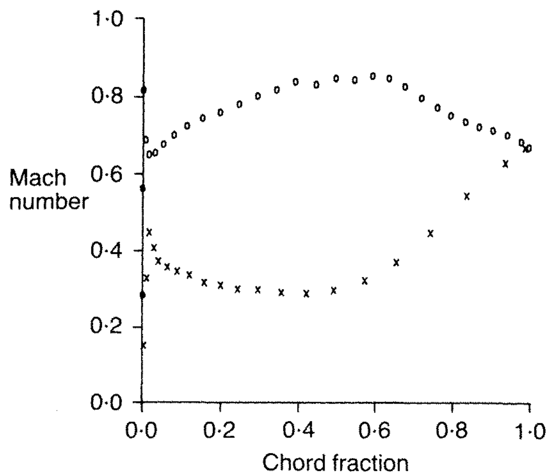

Figure 14. Analysis of turbine blade with leading edge spike

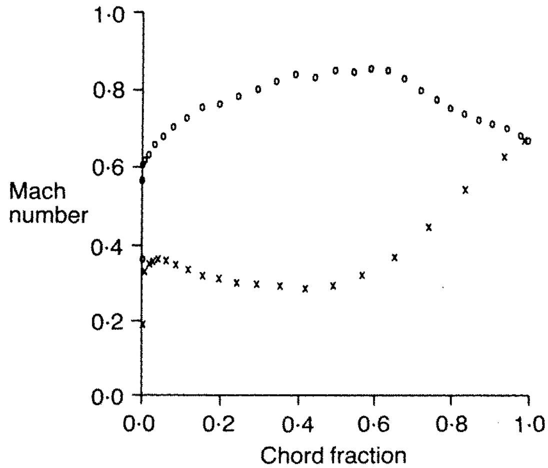

Figure 15. Redesigned blade to remove leading edge spike

4. *Turbine blade leading edge design*

In the past little consideration has been given to the design of blade leading edges. In fact in many methods, both design and analysis, a leading edge cusp is introduced. With such an approach no detailed information is available in this region and often a leading edge circle is fitted for the purpose of blade manufacture. It is known that the leading edge surface velocity distribution can have an important effect on boundary layer transition and separation and hence blade efficiency. The work of Hodson[10] has shown that a 'spike' in the velocity distribution on the leading edge of the suction surface can result in a boundary layer separation bubble.

In this example the analysis of a turbine blade shows the presence of a leading edge spike (see Figure 14). Figure 15 shows the Mach number distribution of the blade after the leading edge spike has been removed. Figure 16 shows the resulting change in geometry from the original blade.

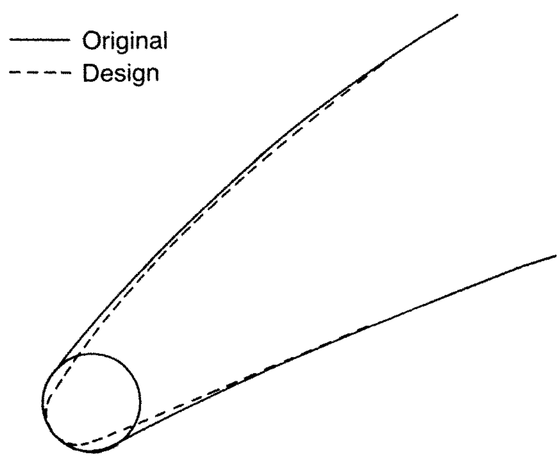

Figure 16. Change in blade shape to remove leading edge spike

CONCLUSIONS

In this paper the mathematical analysis of a finite element compatible design and analysis method is presented. In the method modifications to the blade shape are modelled by transpiring fluid through the blade surface rather than changing the actual geometry; this is an efficient process that does not require the finite element mesh to be reconstructed. The relationship between the velocity distribution and the blade shape is found by 'displacing' each element on the blade surface individually. With a Newton–Raphson formulation and transpiration to model the displacement of each element, this relationship can be determined very efficiently. The 'influence' matrix resulting from this procedure is inverted to determine the blade displacement required to give the desired velocity distribution. The formation of an 'influence' matrix is not confined to the finite element method described and could be incorporated into other blade-to-blade methods. Examples of the use of the method are shown demonstrating its ability to redesign transonic blades with shocks, and blade leading edges.

ACKNOWLEDGEMENT

The authors wish to thank Rolls-Royce Limited for permission to publish this work, and Dr. D. S. Whitehead for his fruitful discussions.

APPENDIX: NOMENCLATURE

- A Element area
- G Global weighting functions
- h Streamtube height
- N Element shape function
- n Distance normal to blade surface
- $\mathbf{R}$ Streamline radius
- S Distance along blade surface
- W Velocity relative to rotating blade

Greek symbols

- κ Blade surface curvature
- ξ Blade surface displacement
- ρ Density
- ϕ Velocity potential
- $\mathbf{\Omega}$ Blade rotation speed

Superscripts

- $\bar{}$ mean value
- $'$ Perturbation to mean value
- m Evaluated at element centroid
- n Evaluated at the nth interation

REFERENCES

1. Chung-Hua Wu, 'A general theory of three-dimensional flow in subsonic and supersonic turbomachines of axial-, radial- and mixed-flow types', *NACA TN2604*, 1952.
2. F. Bauer, P. Garabedian and D. Korn, *Supercritical Wing Sections III*, Lecture notes in economics and mathematical systems, Vol. 150, Springer-Verlag, New York 1975.
3. J. D. Stanitz, 'Design of two-dimensional channels with prescribed velocity distributions along the channel walls', *NACA Rep No 1115*, 1953.
4. E. Schmidt, 'Computation of supercritical compressor and turbine cascades with a design method for transonic flows', *ASME 79-GT-30*.
5. D. S. Whitehead, 'The calculation of steady and unsteady transonic flow in cascades', *Cambridge University Engineering Department CUED/A-Turbo/TR118*, 1982.
6. D. S. Whitehead and S. G. Newton, 'A finite element method for the solution of two-dimensional transonic flows in cascades', *Int. j. numer. methods fluids*, **5**, 115–132 (1985).
7. R. D. Cedar and P. Stow, 'The addition of quasi-three-dimensional terms into a finite element method for transonic turbomachinery blade-to-blade flows', *Int. j. numer. methods fluids*, **5**, 101–114 (1985).
8. H. Rechter, P. Schimming and H. Starken, 'Design and testing of two supercritical compressor cascades', *ASME 79-GT-11*.
9. H. Sobieczky and D. S. Dulikravich, 'A computational design method for transonic turbomachinery cascades', *ASME 82-GT-117*.
10. H. P. Hodson, 'Boundary layer transition and separation near the leading edge of high speed turbine blades', *ASME Paper 84-GT-241*.